Conjugation Chemistry and Bioapplications of Semiconductor Box Nanocrystals Prepared via Dendrimer Bridging

Wenzhuo Guo,[†] J. Jack Li,[†] Y. Andrew Wang,[†,‡] and Xiaogang Peng*[,†]

Department of Chemistry and Biochemistry, University of Arkansas, Fayetteville, Arkansas 72701, and Nanomaterials and Nanofabrication Laboratories (NN-Labs), Fayetteville, Arkansas 72704

Received May 9, 2003

A new strategy, dendrimer bridging, is developed for simultaneous formation and functionalization of biocompatible and bioaccessible semiconductor box nanocrystals—a dendron box around each colloidal semiconductor nanocrystal. CdSe plain core or CdSe/CdS core/shell nanocrystals coated by a monolayer of organic dendron ligands (dendron nanocrystals) with hydroxyl groups as the terminal were chosen as the starting systems because of their potential biocompatibility and proven stability. A generation-two (G2) amine-terminated dendrimer was used as the cross-linking and functionalization reagent, which yielded much more stable cross-linked nanocrystals than the simple diamine or trisamine cross-linking reagents did. The chemical, thermal, and photochemical stability of the resulting amine-terminating box nanocrystals (amine box nanocrystals) formed by dendrimer bridging are comparable to that of the first generation box nanocrystals, achieved by ring-closing metathesis (RCM), that are not biocompatible and need to be further functionalized for bioapplications. As expected, the amine groups on the surface of the box nanocrystals provide versatile and reliable conjugation chemistry under mild conditions. Using one of the conjugation methods, biotin molecules were readily coupled onto the amine box nanocrystals. The biomedical applications of those superstable box nanocrystals were demonstrated by the quantitative and reproducible precipitation of the picomole amounts of avidin with the biotinylated box nanocrystals. Experimental results further revealed that the amine box nanocrystals and related derivatives are fully biocompatible to the tested system, have no detectable nonspecific binding, are extremely stable in the desired bioenvironment, and have no noticeable interference with the bioactivities. The exceptional thermal stability further warrants those biocompatible box nanocrystals to be employed in a large temperature range needed for certain applications, such as PCR.

Introduction

Labeling biological targets with organic fluorophores is a common method for biomedical detections, such as immunoassay and biological imaging techniques. The limitations of most organic dyes include narrow excitation bands, broad emission spectra with a long tail at red wavelength, low photochemical stability, and sophisticated synthetic chemistry.[1] Those limitations make organic dyes not ideal for certain applications, such as multiplexed biological tracking. To complement organic fluorophores, colloidal semiconductor nanocrystals were introduced as alternative choices in 1998.[1,2]

The band-edge photoluminescence (PL) emissions of high-quality semiconductor nanocrystals are narrow, symmetric, and strongly size-dependent due to quantum confinement effects.[3−5] Although the absorption onset also shifts to blue as the size of the nanocrystals decreases, the absorption spectra of nanocrystals with different sizes all extend from the onset to deep UV. These spectral features make it possible to carry out multiple labeling with a single-laser setup. Core/shell nanocrystals formed by growing a lattice-matched, higher band gap material on the top of the core are quite stable against photo-oxidation.[6−9] With the recent developments in synthetic chemistry, nearly monodisperse, highly luminescent semiconductor plain core[10−15]

* To whom correspondence should be addressed. Phone: 479-575-4612. Fax: 479-575-4049. E-mail: xpeng@comp.uark.edu.
[†] University of Arkansas.
[‡] Nanomaterials and Nanofabrication Laboratories.

(1) Bruchez, M.; Moronne, M.; Gin, P.; Weiss, S.; Alivisatos, A. P. *Science* **1998**, *281*, 2013−2016.
(2) Chan, W. C. W.; Nie, S. M. *Science* **1998**, *281*, 2016−2018.
(3) Brus, L. *J. Phys. Chem.* **1986**, *90*, 2555−60.
(4) Alivisatos, A. P. *Science* **1996**, *271*, 933−937.
(5) *Acc. Chem. Res.* **1999**, *32* (Special Issue for Nanostructures), review articles relevant to colloidal nanocrystals.
(6) Hines, M. A.; Guyot-Sionnest, P. *J. Phys. Chem.* **1996**, *100*, 468−471.
(7) Peng, X.; Schlamp, M. C.; Kadavanich, A. V.; Alivisatos, A. P. *J. Am. Chem. Soc.* **1997**, *119*, 7019−7029.
(8) Dabbousi, B. O.; RodriguezViejo, J.; Mikulec, F. V.; Heine, J. R.; Mattoussi, H.; Ober, R.; Jensen, K. F.; Bawendi, M. G. *J. Phys. Chem. B* **1997**, *101*, 9463−9475.
(9) Li, J.; Wang, Y. A.; Guo, W.; Peng, X., submitted.
(10) Peng, Z. A.; Peng, X. *J. Am. Chem. Soc.* **2001**, *123*, 183−184.
(11) Qu, L.; Peng, Z. A.; Peng, X. *Nano Lett.* **2001**, *1*, 333−337.
(12) Qu, L.; Peng, X. *J. Am. Chem. Soc.* **2002**, *124*, 2049−2055.
(13) Peng, Z. A.; Peng, X. *J. Am. Chem. Soc.* **2002**, *124*, 3343−3353.

10.1021/cm034341y CCC: $25.00
Published on Web 07/10/2003

and core/shell[9] nanocrystals covering an entire optical window could be prepared at low cost with so-called greener approaches. All those features have attracted tremendous interest in exploring biomedical applications using semiconductor nanocrystals.

The main challenge in the biomedical application is the availability of stable water-soluble nanocrystals. This is so because of the unreliable binding between inorganic nanocrystals and their surface organic ligands. Inorganic nanocrystals are metastable species and need to be kinetically stabilized generally through a monolayer of organic ligands on their surface. This monolayer of organic ligands also provides binding sites for the outside world, related to this work, biomedical functional groups. Thus, the detachment of organic ligands from their inorganic nanocrystal cores will make nanocrystals lose their biomedical functions, be chemically or photochemically etched, form aggregates, and precipitate from the solution.

As-prepared semiconductor nanocrystals in most cases are capped with hydrophobic organic ligands. For biomedical applications, those hydrophobic ligands are replaced or wrapped by hydrophilic ligands. Since studies on ligand chemistry of nanocrystals are still very rare,[16] the surface modification and functionalization of nanocrystals have been mostly performed empirically. Many interesting and innovative ideas, such as silica coating,[1,17,18] natural[19] and synthetic polymer[20,21] wrapping via either ionic interaction or van der Waals interaction, micelle capping,[22] and simple ligand replacement,[2,23] have been reported recently to solve this critical problem.

Our approach to solve the ligand chemistry issue is based on the understanding of the mechanisms of the photochemical instability of semiconductor nanocrystals[16] identified by a systematic study. The mechanisms indicate that a dense ligand monolayer with strong interligand interactions should improve the photochemical, chemical, and thermal stability. The ligands designed by us are so-called organic dendrons,[24] which are regularly branched organic molecules with a focal point as the binding site to the surface of nanocrystals. The cone shape packing and the interligand chain tangling within the ligand monolayer were proven to greatly improve the photochemical stability of semiconductor nanocrystals. Those dendron-coated nanocrystals (dendron nanocrystals) are structurally simple and the corresponding ligand monolayer is very thin in comparison to other stabilization approaches. The multiple terminal groups of each dendron, typically eight or more for a generation-3 (G3) dendron, render one-step further stabilization of nanocrystals, that is, to globally cross-link all the ligands on the surface of a nanocrystal to form box nanocrystals.[25] The first example of box nanocrystals was demonstrated through ring-closing metathesis (RCM) of the terminal double bonds of G3 dendron ligands.[25] The stability of those box nanocrystals against harsh chemical, photochemical, and thermal treatments is superior, which are likely ideal structures for many purposes. However, those double bond-terminated box nanocrystals are insoluble in water and substantial efforts are needed to develop desired coupling strategies for biomedical applications using those box nanocrystals.

This work was intended to develop a class of bioaccessible and biocompatible box nanocrystals using high-quality semiconductor nanocrystals, including plain core and core/shell nanocrystals. To fulfill this goal, a new cross-linking strategy was introduced, dendrimer bridging. This new strategy forms a water-soluble dendron box around each particle and functionalizes it simultaneously. The resulting amine dendrimer-bridged box nanocrystals (amine box nanocrystals) are extremely stable against chemical, thermal, and photochemical treatments. The surface amine groups provide simple, reliable, and versatile coupling methods for biomedical and chemical purposes. As an example, biotin molecules were coupled to the amine box nanocrystals. The resulting biotinylated box nanocrystals are resistant to nonspecific binding and stable against chemical, photochemical, and biochemical treatments. A simple but quantitative and reproducible detection scheme for avidin was demonstrated using those biotinylated box nanocrystals.

Experimental Section

Chemicals. Triphenylmethanol, 2-aminoethanethiol hydrochloride, bromoactyl bromide, triethylsilane, trifluoroacetic acid (TFA), tetramethylammonium hydroxide, *N*,*N*′-disuccinimidyl carbonate (DSC), 4-cyanobenzaldehyde, 4-cyanobenzoic acid, succinic anhydride, 4-(dimethylamino)pyridine (DMAP), ethylenediamine, trioctylphosphine oxide (TOPO, technical grade, 90%), trioctylphosphine (TOP, technical grade, 90%), cadmium acetate hydrate (99.99+%), selenium powder (100 mesh, 95%), anhydrous toluene (99.8%), and anhydrous methyl sulfoxide (DMSO) were purchased from Aldrich. Tris(2-aminoethyl)amine was purchased from Lancaster. Immunopure avidin and sulfo-NHS-biotin were purchased from Pirece. Anhydrous ethyl ether, benzene, chloroform, *N*,*N*-dimethylformamide (DMF), acetone, ethyl acetate, methanol, triethylamine, and K_2CO_3 were purchased from EM science and used directly without further purification.

Synthesis of G3-OH Dendron Ligand-Coated Nanocrystals. CdSe and CdSe/CdS core/shell nanocrystals coated with hydrophobic ligands were synthesized following standard procedures.[9,16] The G3-OH dendron ligand (Chart 1) was synthesized following a procedure previously described with few modifications.[24]

The surface replacement of the original ligands by G3-OH dendrons was achieved using the two-phase approach reported

(14) Yu, W. W.; Peng, X. *Angew. Chem. Int. Ed.* **2002**, *41*, 2368−2371.
(15) Battaglia, D.; Peng, X. *Nano Lett.* **2002**, *2*, 1027−1030.
(16) Aldana, J.; Wang, Y.; Peng, X. *J. Am. Chem. Soc.* **2001**, *123*, 8844−8850.
(17) Gerion, D.; Pinaud, F.; Williams, S. C.; Parak, W. J.; Zanchet, D.; Weiss, S.; Alivisatos, A. P. *J. Phys. Chem. B* **2001**, *105*, 8861−8871.
(18) Gerion, D.; Parak, W. J.; Williams, S. C.; Zanchet, D.; Micheel, C. M.; Alivisatos, A. P. *J. Am. Chem. Soc.* **2002**, *124*, 7070−7074.
(19) Mattoussi, H.; Mauro, J. M.; Goldman, E. R.; Anderson, G. P.; Sundar, V. C.; Mikulec, F. V.; Bawendi, M. G. *J. Am. Chem. Soc.* **2000**, *122*, 12142−12150.
(20) Wu, X.; Liu, H.; Liu, J.; Haley, K. N.; Treadway, J. A.; Larson, J. P.; Ge, N.; Peale, F.; Bruchez, M. P. *Nature Biotechnol.* **2003**, *21*, 41−46.
(21) Potapova, I.; Mruk, R.; Prehl, S.; Zentel, R.; Basche, T.; Mews, A. *J. Am. Chem. Soc* **2003**, *125*, 320−321.
(22) Dubertret, B.; Skourides, P.; Norris, D. J.; Noireaux, V.; Brivanlou, A. H.; Libchaber, A. *Science* **2002**, *298*, 1759−1762.
(23) Pathak, S.; Choi, S.; Arnheim, N.; Thompson, M. E. *J. Am. Chem. Soc.* **2001**, *123*, 4103−4104.
(24) Wang, Y. A.; Li, J. J.; Chen, H.; Peng, X. *J. Am. Chem. Soc.* **2002**, *124*, 2293−2298.
(25) Guo, W.; Li, J.; Wang, Y. A.; Peng, X. *J. Am. Chem. Soc. 125*, 3901−3909.

Chart 1. Structures of Four Key Compounds Used in This Work

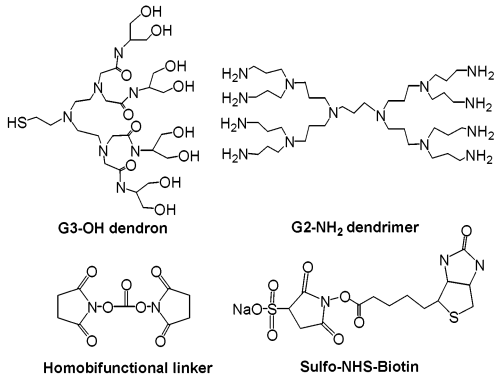

previously.[24] An alternative two-phase procedure was developed to modify initially amine-coated CdSe/CdS core/shell nanocrystals. Typically, 150 mg of dendron ligands was dissolved in 15 mL of 1:1 ratio MeOH/$CHCl_3$ solution, and the pH value of such solution was set to 10.3 by addition of tetramethylammonium hydroxide. To this basic dendron ligand solution was added 20 mg of nanocrystals. After the reaction mixture was stirred for 4 h, 2 mL of water and 2 mL of MeOH were added in order. Two phases formed eventually with slight shaking. The upper layer with nanocrystals dissolved in it was then transferred to another vial and kept overnight. The resulting dendron nanocrystals were precipitated out with ethyl ether and acetone, separated by centrifugation and decantation. The dissolving and precipitation procedure was repeated at least three times to remove free ligands. The final product was dried under vacuum for 2 h, and the resulting power was dissolved in anhydrous methyl sulfoxide (DMSO) for cross-linking.

Formation of Amine Terminated Box Nanocrystals via Dendrimer Bridging (Scheme 1). Homobifunctional cross-linker, *N*,*N*-disuccinimidyl carbonate (DSC, 8 mg), and 4-(dimethylamino)pyridine (DMAP, 6 mg) were added to a 15-mL solution of G3-OH-coated nanocrystals in dry DMSO. The absorbance at the first exciton peak of the nanocrystals solution was 1.26. After the solution was stirred overnight, 2 mL of such solution was added dropwise into 15 mL of DMF solution containing 8 mg of G2 dendrimer amine (structure in Chart 1). The resulting precipitates were isolated by centrifugation and washed with water three times. The final amine-terminated box nanocrystal was dissolved in HCl solution (pH = 2) and immediately neutralized with aqueous NaOH to pH around 7. The amine box nanocrystal solutions were kept dispersible between pH = 2 and pH = 9.

A similar cross-linking procedure was applied using ethylenediamine or tris(2-aminoethyl)amine, instead of G2 dendrimer amines. Different from the products obtained via the dendrimer bridging, nanocrystals with diamine or trisamine as the linkage reagents were soluble in the coupling solutions. The resulting cross-linking products were used as references for the stability studies.

Photochemical, Chemical, and Thermal Stability of Box Nanocrystals. The photochemical stabilities were studied following the previously reported procedure.[24] The aqueous nanocrystal solutions with absorbance of the first absorption peak to ~0.3 were placed about 4 cm under an ultraviolet lamp (UVP model UVGL-25 multiband, 254 nm used) in air. The UV−vis absorption spectra (UV−vis and PL spectra for core/shell nanocrystals) were monitored at certain time intervals. The absorbance at the original excitation absorption peak or the PL intensity was used as the indicator of photo-oxidation processes.

Two types of chemical stabilities of nanocrystals were investigated, that is, HCl etching and H_2O_2 oxidation. In a typical HCl etching experiment, nanocrystals were dissolved in HCl solution (pH = 1) in a cuvette with the initial absorbance at the first absorption peak of the nanocrystals around 0.5. The UV−vis spectra were recorded at a certain time interval until the solution became turbid. The H_2O_2 oxidation experiments were carried out similarly to the HCl etching, but with H_2O_2 (0.1 mL, 3 wt % in water) as oxidant.

The thermal stability of nanocrystals was examined by sintering the nanocrystals. The purified samples were placed in a vacuum oven and dried and degassed for 2 h prior to heating. The oven temperature was raised to 100 °C and kept at that temperature for about 150 min. After the oven was cooled to ambient temperature, the solubility of the resulting fine powder was tested, and the UV−vis absorption spectra of the solutions were recorded.

Coupling Chemistry of the Amine Box Nanocrystals. Amine box nanocrystals were found to be very versatile for surface coupling reactions (Scheme 2). Coupling reagents such as 4-cyanobenzaldehyde (2.5 mg) in 5 mL of DMSO or dioxane was added to the solution of amine box nanocrystals with the absorbance of the first absorption peak of the nanocrystals at 2.5. The pH value of such solution was adjusted to 8. After overnight stirring, the nanocrystals were precipitated out with a minimum amount of ethyl ether and acetone, separated by centrifugation and decantation. The resulting nanocrystal was then redissolved and precipitated with the suitable solvents system, separated by centrifugation and decantation at least three times to remove excess reagents. The final nanocrystal products were characterized by IR measurements by casting the nanocrystals solution on to the CaF_2 IR window. Other methods were also applied to characterize the final products, such as UV−vis for the Schiff base formation.

Couple Biotin Molecules onto Amine Box Nanocrystals To Form Biotinylated Box Nanocrystals. Sulfo-NHS-biotin (2 mg) was added to 4 mL of amine box nanocrystal solution in H_2O and DMSO solvent (1:1). The absorbance of the first absorption peak of the nanocrystals in the solution was 2.5. After overnight stirring at room temperature, the slight turbid solution was centrifuged. The top clear solution was decanted to another vial for the bioassay. The amount of precipitates was found to be dependent on the ratio of biotin to the box nanocrystals. It was observed that a high density of biotin on the surface of box nanocrystals made them insoluble in either pure water or mixture solvent containing water.

Avidin Detection Using Biotinylated Box Nanocrystals. Conjugation of biotinylated box nanocrystals with avidin was carried out by addition of 10 μL of avidin solution (1 mg/mL in PBS buffer) to an optical cuvette containing 0.5 mL of biotinylated box nanocrystals with absorbance around 0.4 at the first absorption peak. The cloudy mixture formed upon the addition was centrifuged for 5 min, and the PL intensity and UV−vis absorbance of the upper clear solution were monitored. The addition of avidin, centrifugation, and monitoring procedure was repeated until there was no more precipitate forming. The precipitate of avidin−biotin/box nanocrystal complexes was denaturized by heating to about 70 °C.

Results and Discussion

CdSe and CdSe/CdS dendron nanocrystals coated with the G3-OH dendron ligand shown in Scheme 1 was chosen as our starting material for the formation of bioaccessible and biocompatible box nanocrystals. Among the 30−50 dendron ligands designed and synthesized by this team, the G3-OH dendron was found to yield dendron nanocrystals with the best photochemical stability[24] because of some yet unknown reasons. In addition to this, the hydroxyl group is considered as a common type of biocompatible functional group, which is water-soluble and has low nonspecific binding for biomolecules.

Activation of the Hydroxyl Groups. Activation of the hydroxyl groups was performed with the homobifunctional linker shown in Chart 1. It is necessary to

Scheme 1. One-Pot Formation of Amine Box Nanocrystals

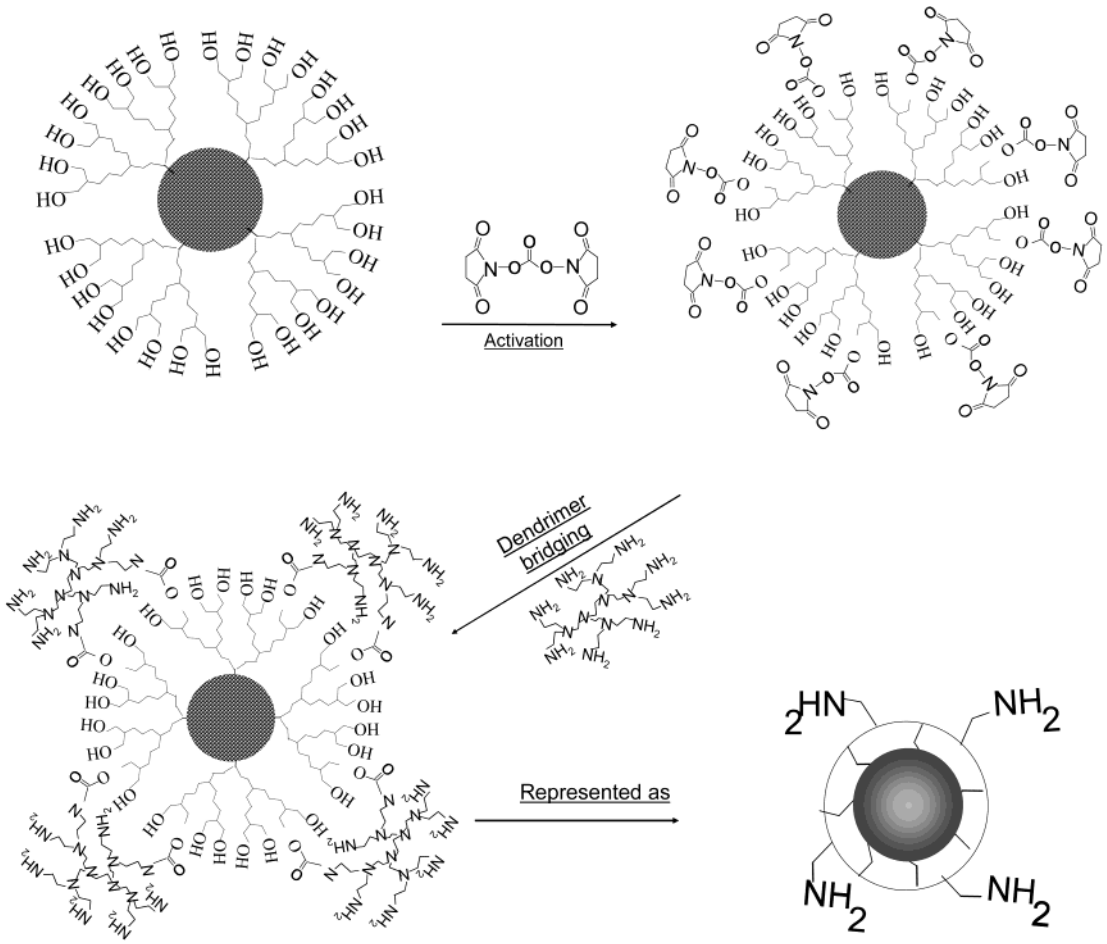

Scheme 2. Summary of Coupling Strategies for Amine Box Nanocrystals

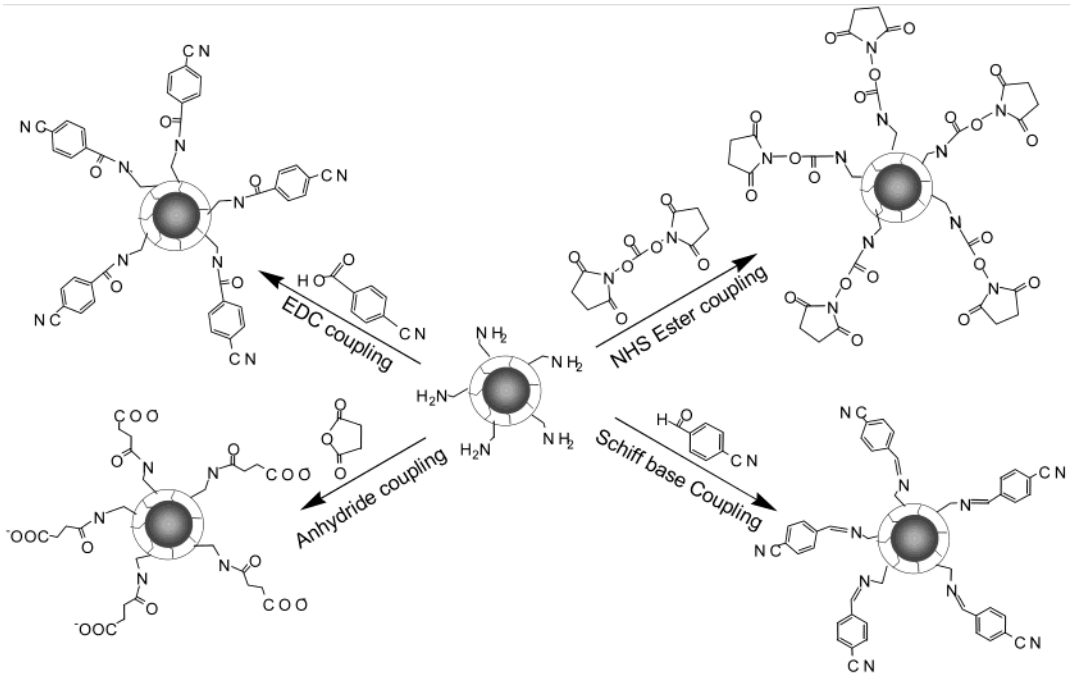

remove the moisture present in the G3-OH dendron-nanocrystal samples. Either vacuum-drying in powder form or drying with 4-Å molecular sieves in solution worked well. The duration of vacuum-drying should be shorter than 2 h; otherwise, it took a long time to redisperse the dendron nanocrystals in DMSO solution. The stability of those over-dried dendron nanocrystals often decreased significantly even if they could be dispersed. For this reason, drying using molecular sieves is preferred. With those dried dendron nanocrystals and

anhydrous DMSO as the solvent, activation of hydroxyl groups with the homobifunctional linker readily took place using DMAP as the catalyst. It is essential to keep a relatively low nanocrystal concentration and use excess reagents to avoid interparticle cross-linking.

Formation of Amine Box Nanocrystals through Dendrimer Bridging. Purification of activated dendron nanocrystals was unnecessary for the subsequent dendrimer-bridging step. The final product of the dendrimer bridging precipitated out of the solution, and control experiments revealed that possible side products and excess reactants were all soluble in the cross-linking solution. In contrast, while either ethylenediamine or trisamine was used as the cross-linking reagent, precipitation of nanocrystals was not observed.

The amine box nanocrystals precipitated from the cross-linking solution must be dispersed in acidic conditions with a pH value around 2, although they remained dispersed in solution after the acidic dispersion was neutralized up to about pH = 9. When the pH value further increased above 10, the amine box nanocrystals flocculated from the solution. Again, this precipitate could be redispersed in acidic conditions and stable in solution at neutral pH values. This interesting dispersion feature of the amine box nanocrystals is probably due to the high surface density of amine groups. Only acidic conditions could break the multiple hydrogen bonds existing between the adjacent nanocrystals.

We tried to characterize the dendron boxes by etching away the inorganic cores. Similar to the box nanocrystals formed using RCM strategy, the widths of ^{1}H NMR peaks did not change upon the removal of the inorganic cores. Although no mass signals for monomers or oligomers of dendron and dendrimer were detected, we did not observe any meaningful mass signals corresponding to the empty dendron box, likely because the molecular mass of the empty dendron boxes was too high to be detected.

The stability results shown in the following section (see Figures 2 and 3) indicate that global cross-linking of G3-OH dendron ligands on each nanocrystal using dendrimer bridging was achieved. However, the desired global cross-linking was not obtained using diamine or trisamine as cross-linking reagents. We think the bulky flexible structure of amine dendrimer caused the difference. Once the amine group of the dendrimer reacted with the activated hydroxyl group, the bulky structure prevented the access of another dendrimer molecule. In doing so, the other flexible amine branches on the same molecule have a higher chance of reaching with the nearby activated hydroxyl groups on the same nanocrystals. The relative small and rigid molecular structures of diamine or trisamine make the cross-linking reactions unfavorable with respect to the competing reaction, the monocoupling events between the activated hydroxyl groups, and free diamines or trisamines present in the solutions. This resulted an insufficient cross-linking.

Amine groups are the most versatile coupling sites for bioconjugation under mild conditions. As demonstrated in Scheme 2, a variety of coupling strategies are applicable if nanocrystals possess amine groups on their surface. However, amine groups are also good binding groups for most of the nanocrystals. It is difficult to obtain amine groups on the nanocrystals surface[26] by the common ligand displacement method. Wrapping as-prepared nanocrystals with multiamine-containing molecules will bridge nanocrystals from each other and destabilize the colloidal dispersion since the ligand monolayer of the nanocrystal is not very dense for the nanocrystals coated by conventional ligands.[26]

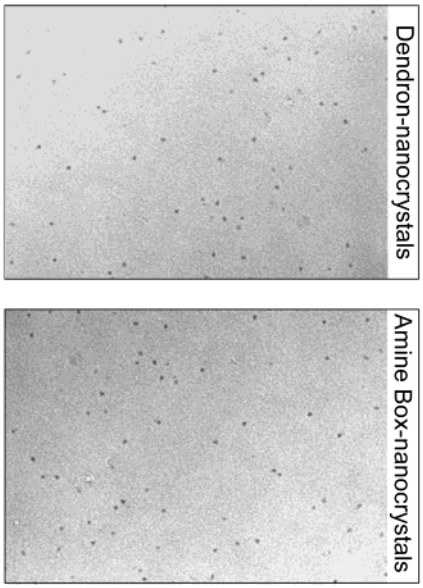

Figure 1. TEM images of 3.5-nm CdSe nanocrystals before (dendron nanocrystals) and after (amine box nanocrystals) the cross-linking reaction.

While the good stability of dendron nanocrystals made it possible for the nanocrystals to withstand some simple reactions necessary for the formation of box nanocrystals, the densely packed ligand monolayer of a dendron nanocrystal further isolates the chemical events that occurred on the outer surface of the ligand monolayer from the interface between the inorganic core and the ligand monolayer. Amine groups brought onto the surface of a given nanocrystal by the dendrimer-bridging process cannot penetrate this densely packed ligand monolayer of other nanocrystals in the solution. Therefore, the resulting amine box nanocrystals are stable as a colloidal dispersion without interparticles cross-linking. We examined the dendron nanocrystals and the resulting amine box nanocrystals under TEM (absorbance of the first absorption peak of nanocrystals in the deposition solution below 0.01). On the basis of simple molecular modeling for 3.5-nm nanocrystals, only those nanocrystals which are separated with a distance roughly equal to or smaller than the size of a nanocrystal could be considered as chemically coupled through either an amine dendrimer or a homolinker. As shown in Figure 1, nanocrystals in both cases are reasonably separated from each other, which suggests that interparticle cross-linking was insignificant.

Stability of Amine Box Nanocrystals. The stability of amine box nanocrystals were quantitatively examined against acid etching, oxidation with H_2O_2, photo-oxidation, and thermal sintering using the methods reported previously.[16,24,25] For comparison, the den-

(26) Peng, X.; Wilson, T. E.; Alivisatos, A. P.; Schultz, P. G. *Angew. Chem. Int. Ed.* **1997**, *36*, 145−147.

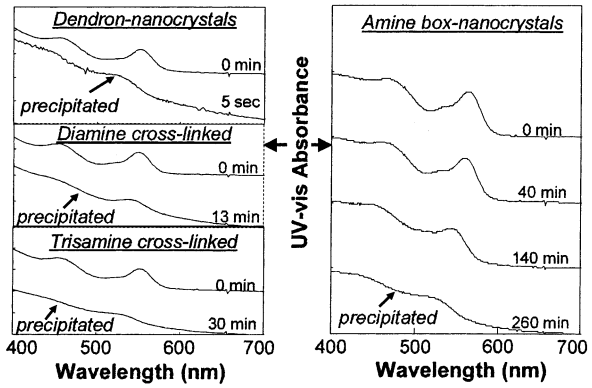

Figure 2. Stability of CdSe nanocrystals with different types of ligand shells against HCl (pH = 1) etching.

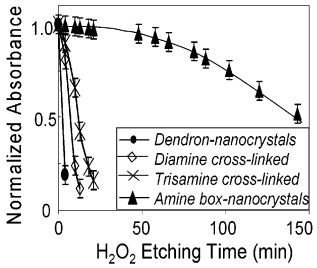

Figure 3. Temporal evolution of the absorbance at the first absorption peak of the nanocrystals upon chemical oxidation. Experiments stopped at the precipitation point of each sample.

dron nanocrystals and their cross-linking products with ethylenediamine and trisamine were also examined.

Upon exposure to HCl solution (pH = 1), G3-OH-coated dendron nanocrystals decomposed immediately and the inorganic nanocrystals precipitated out of the solution in 5 s. However, it took more than 4 h for amine box nanocrystals to precipitate, and the absorption spectrum of the inorganic cores did not show any significant blue shift within 40 min of the exposure. The two controls, the diamine and trisamine cross-linked dendron nanocrystals, were more stable than their mother dendron nanocrystals but much less stable than the amine box nanocrystals (Figure 2).

The amine box nanocrystals were much more stable against chemical oxidation in H_2O_2 aqueous solution (0.15 mol/L) than the dendron nanocrystals with or without cross-linking by diamine and trisamine. Figure 3 illustrates the temporal evolution of the absorbance at the first absorption peak of the nanocrystals in the H_2O_2 solutions. For the dendron nanocrystals, with or without diamine/trisamine cross-linking, oxidation of the nanocrystal cores was immediately detected and the precipitation of the inorganic nanocrystals occurred within 25 min. The oxidation of the inorganic cores of the amine box nanocrystals was slowly observed, and the precipitation of the nanocrystals occurred after the oxidation proceeded for about 140 min.

The thermal stability of the amine box nanocrystals was found to be superior, even in comparison to the box nanocrystals made by RCM.[25] After sintering for 150 min, the optical properties of the box nanocrystals remained (Figure 4, left). The exceptional thermal stability of the amine box nanocrystals warrants their possible biomedical applications at elevated tempera-

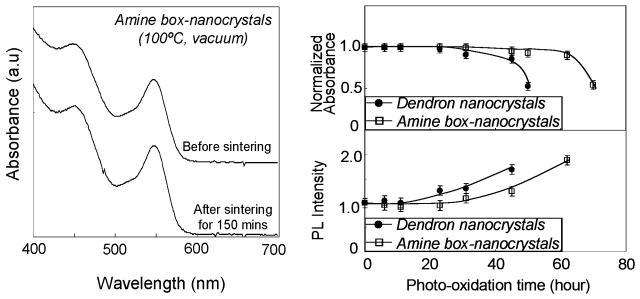

Figure 4. Left: UV−vis spectra of amine box nanocrystals before and after sintering at 100 °C for 150 min. **Right:** Photo-oxidation of CdSe/CdS core/shell amine box nanocrystals and the corresponding dendron nanocrystals under UV radiation in air.

tures. For instance, they may be used as marks for PCR-related techniques.

The photochemical stability of amine box nanocrystals was significantly improved in comparison to the corresponding dendron nanocrystals—the most stable dendron nanocrystals obtained up to present. Figure 4 (right) illustrates the experimental results for the amine box nanocrystals with CdSe/CdS core/shell nanocrystals as the inorganic component. Under the same photo-oxidation conditions, the amine box nanocrystals precipitated out in about 72 h while it took 48 h for the corresponding dendron nanocrystals to precipitate out of the aqueous solution.

Generally, the stability of the amine box nanocrystals formed by dendrimer bridging is more or less compatible with that of the box nanocrystals formed by RCM reactions[25] (compare Figures 2, 3, and 4 to the corresponding results in the previous work). The chemical stability against either HCl or H_2O_2 and the thermal stability of the amine box nanocrystals were better than those of the previously reported ones.[25] The improvement of the photochemical stability of the amine box nanocrystals was not as dramatic as the one reported previously. It should be pointed out that photo-oxidation in water—the solvent for amine box nanocrystals—typically occurred faster than that in organic solvents.[9]

Optical Properties of Amine Box Nanocrystals. The optical properties of amine box nanocrystals were very similar to those of their corresponding dendron nanocrystals. If the box nanocrystals were made with plain CdSe core nanocrystals, the nanocrystals did not show any band edge emission. For CdSe/CdS core/shell nanocrystals, the photoluminescence (PL) brightness of box nanocrystals was about the same as their corresponding dendron nanocrystals. Upon photo-oxidation, the PL brightness of both dendron nanocrystals and box nanocrystals increased significantly (Figure 4).

Coupling Chemistry of Amine Box Nanocrystals. The coupling chemistry of amine box nanocrystals was found to be diverse and to readily occur with high yields. Scheme 2 illustrates four different coupling strategies commonly used in bioconjugation. Since the NMR spectra of colloidal nanocrystals are inevitably broad and typically not informative,[16] we chose FTIR as the monitoring means like we did for the dendron nanocrystals.[24] To do so, reagents with distinguishable IR fingerprints were employed for the model coupling reactions. Figure 5 illustrates the FTIR spectra of the dendron nanocrystals, amine box nanocrystals, and the

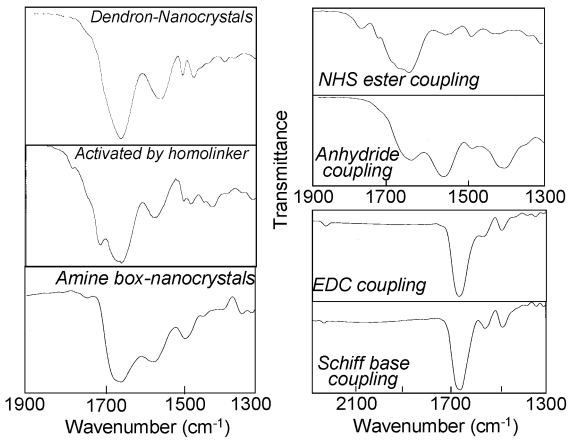

Figure 5. FTIR spectra of nanocrystal/ligand complexes. Left: Formation of amine box nanocrystals. Right: Coupling products of the amine box nanocrystals via different coupling reactions shown in Scheme 2.

coupling products of the box nanocrystals resulting from different coupling reactions. The assignments of the IR fingerprint peaks[27] are provided in Table 1. Coupling reactions with small molecule analogues were also carried out and the IR spectra of the purified products were recorded for reference.

N-Hydroxylsuccinimide (NHS) ester is probably the most common activation chemistry for creating reactive acylating reagents. The majority of amine-reactive cross-linking or modification reagents commercially available utilize NHS ester. *N*,*N*-Disuccinimidyl carbonate (DSC) was employed to testify this kind of reactivity. The reaction could be easily followed by IR spectra shown in Figure 5. The band at around 1567 cm^{-1}, assigned to $-NH_2$ deformation and amide II, became much weaker after the reaction. In addition, two new bands at 1770 and 1731 cm^{-1} corresponding to ester carbonyl and NHS carbonyl stretching vibration, respectively, appeared after the coupling reaction.

Carbonyl groups such as aldehydes and ketones can react with amine to form Schiff base. This chemistry is widely applied to modify protein or peptide with reducing sugar such as glucose. An aromatic aldehyde, 4-cyanobenzaldehyde, which forms a relative stable aromatic Schiff base, was selected to react with amine box nanocrystals. One of the IR signatures of this coupling reaction is the high intensity of the band centered at 1655 cm^{-1} assigned as a combination of amide I band from G3-OH ligand and C═N stretching of the Schiff base. This spectral feature along with the appearance of the characteristic cyano stretching vibration at 2226 cm^{-1} and the disappearance of the NH_2 deformation band at 1567 cm^{-1} all confirmed the formation of Schiff base. It is also well-known that Schiff base is UV-active. This was identified as the color change of the solution, from the red-orange color of the nanocrystal solution gradually to yellow. This color change was also evidenced by the appearance of a strong absorption peak at around 440 nm (Figure 6, bottom). To further confirm the formation of Schiff base, a control experiment was carried out using G2-NH_2 dendrimer and 4-cyanobenzaldehyde. The UV−vis spectrum of the resulting compound is shown in Figure 6 (top), which possesses a strong and broad absorption peak at 440 nm. It should be pointed out that the Schiff base formed in this case was not ultimately stable. Upon aging in air for days, the yellow color of the solution gradually faded back to orange-red color of the original nanocrystal solutions.

The amine box nanocrystals underwent carbodiimide-mediated amide bond formation with carboxylic acid. This kind of reaction was demonstrated by EDC coupling between amine box nanocrystals and 4-cyanobenzoic acid. The IR signatures of the resulting products were very similar to that of the Schiff base because of the similarity of the products.

The nucleophilic attack of surface amine groups to acid anhydride also worked well, which yielded amide bonds and free carboxylate groups. Under basic conditions, the surface carboxylate groups made the resulting nanocrystals negatively charged. The IR signature of carboxylate anions were observed, with the symmetric vibration at around 1400 cm^{-1} and the asymmetric one at 1550 cm^{-1} (Figure 5).

Bioaccessibility of the Amine Box Nanocrystals. The bioaccessibility of the amine box nanocrystals was further demonstrated by coupling biotin onto the surface of the nanocrystals using one of the above demonstrated coupling strategies, NHS ester coupling. The resulting nanocrystals are tentatively named as biotinylated box nanocrystals. The commercially available Sulfo-NHS-biotin worked well in reacting with the amine box nanocrystals. The reaction was carried out for a relatively long time to reduce the free biotin reagent in the system. By doing so, further separation of resulting biotinylated box nanocrystals was unnecessary. With more biotin units on each nanocrystal surface, the original hydrophilic box nanocrystal gradually became hydrophobic due to the poor hydrophilic nature of the biotin reagent. The biotinylated box nanocrystals with high biotin density on the surface precipitated out from the typical reaction solution (DMSO:H_2O equals 1:1). Therefore, the amount of biotin on each nanocrystal should be controlled in such a manner that the nanocrystal reserves the solubility and, at the same time, exhibits a maximum number of binding sites for avidin.

The biotinylated core/shell box nanocrystals exhibit the same stability as amine box nanocrystals. For example, the PL intensity of biotinylated core/shell box nanocrystals were kept constant for hours under the standard photo-oxidation conditions, and for at least several months under ambient conditions. The excellent stability of bioconjugated box nanocrystals provides an essential base for quantitative binding assays to be developed using biofunctional box nanocrystals.

Biomedical Applications. Biomedical applications of the box nanocrystals were demonstrated using a biotin−avidin binding assay with biotinylated box nanocrystals. Avidin is a glycoprotein which contains four identical subunits. Each subunit possesses one binding site for one biotin molecule. The strong but noncovalent binding between avidin and biotin makes it extraordinarily useful in bioconjugation chemistry. The biospecificity of the interaction is similar to antibody−antigen or receptor−ligand recognition, but on a much higher level with respect to affinity constant.

(27) Silverstein, R. M.; Bassler, G. C.; Morrill, T. C. *Spectrometric Identification of Organic Compounds*; Wiley-VCH: New York, 1991.

Table 1. IR Signatures[27] of the Dendron Nanocrystals, Amine Box Nanocrystals, and Coupling Products of the Amine Box Nanocrystals (See Structures in Scheme 2)

species	fingerprint peaks (cm^{-1})	assignments
G3-OH dendron nanocrystals	1661	C═O stretching vibration (amide I)
	1566	N−H bending vibration (amide II)
activated G3-OH	1774	C═O stretching vibration (ester)
dendron nanocrystals by homolinker	1669	C═O stretching vibration (NHS amide I)
	1655	C═O stretching vibration (amide I)
	1556	N−H bending vibration (amide II)
amine box nanocrystals	1670	C═O stretching vibration (amide I)
	1567	NH2 deformation and N−H bending vibration
NHS ester coupling product	1770	C═O stretching vibration (ester)
	1731	C═O stretching vibration (NHS amide I)
	1664	C═O stretching vibration (amide I)
	1556	N−H bending vibration (amide II)
anhydride coupling product	1651	C═O stretching vibration (amide I)
	1550	carboxylate ion asymmetrical stretching
	1400	carboxylate ion symmetrical stretching
EDC coupling product	2226	C≡N stretching
	1661	C═O stretching vibration (amide I)
	1549	N−H bending vibration (amide II)
Schiff base coupling product	2226	C≡N stretching
	1655	C═N and C═O stretching vibration (amide I)
	1553	N−H bending vibration (amide II)

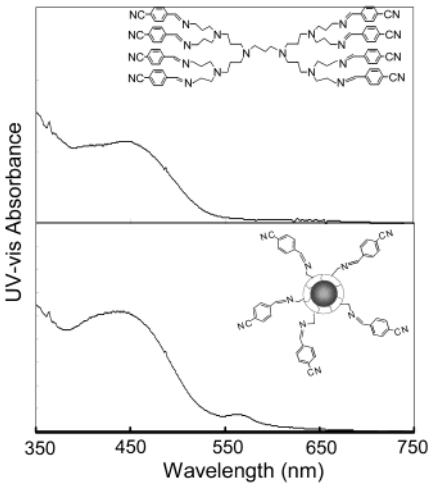

Figure 6. UV−vis spectra of Schiff base formed with free dendrimer (top) and amine box nanocrystals (bottom). The peak at 560 nm (bottom) is due to the absorption of nanocrystals.

Upon the addition of a certain amount of avidin (75 pmol) in PBS buffer to the biotinylated box nanocrystals in DMSO and H_2O solution (1:1 ratio), the clear solution turned to turbid immediately, indicating the formation of avidin−biotin/box nanocrystal conjugates. This turbid solution was centrifuged for a few minutes to obtain a clear top solution for UV−vis and PL measurements. The addition of avidin was continued until the solution was almost colorless. Figure 7 (left) schematically demonstrates the chemical processes, and the right panel shows the results of the UV−vis and PL measurements. A picomole amount of avidin could be readily detected, and the results from both UV−vis and PL measurements of two parallel detection reactions were almost identical.

As shown in Figure 7, the PL intensity dropped about 60% after the first addition of avidin, and the UV−vis absorbance only dropped about 20%. This discrepancy between two measurements revealed some different natures of PL and UV−vis measurements. At relatively low avidin concentrations, there must be some small aggregates of nanocrystals formed by the avidin−biotin binding. Those small aggregates were dispersible in the solution and could not be precipitated by the relatively slow centrifugation applied in this work. As a result, they contributed to the UV−vis signal. However, when several particles in those small aggregates were only isolated from each other by a distance not much larger than the size of one particle, PL of those nanocrystals would be significantly quenched because of re-absorption, Forster energy transfer, and so forth. The final result of these two effects should make the change of the UV−vis reading to be significantly lower than that of the PL one.

Nonspecific Binding. Nonspecific binding of the box nanocrystals to biological targets was also studied since it was observed previously.[1] Three sets of experiments were performed to exclude nonspecific binding in this system. In the first control experiment, the same volume of PBS buffer without avidin was added into the biotinylated box nanocrystal solution, and no precipitate was observed. The UV−vis absorbance and PL intensity after calibration of dilution effect were kept as constants with repeated centrifugation and addition of the buffer solution (Figure 7). This result revealed that the biotinylated box nanocrystals are stable in the buffer solution.

The second control experiment was designed to study the nonspecific binding of avidin with the amine groups on the surface of the box nanocrystals. The same amount of avidin was added to the solution of amine box nanocrystals under exactly the same conditions for the biotinylated box nanocrystal system. Again, no precipitation was observed using the amine box nanocrystals, and no change of either UV−vis absorbance or PL intensity was observed during the continuous addition of the avidin solution (Figure 7). These results indicate that the box nanocrystals did not show any significant nonspecific binding in this system.

The third experiment was designed to directly verify that the precipitation of the nanocrystals observed in Figure 7 was indeed due to the specific binding between

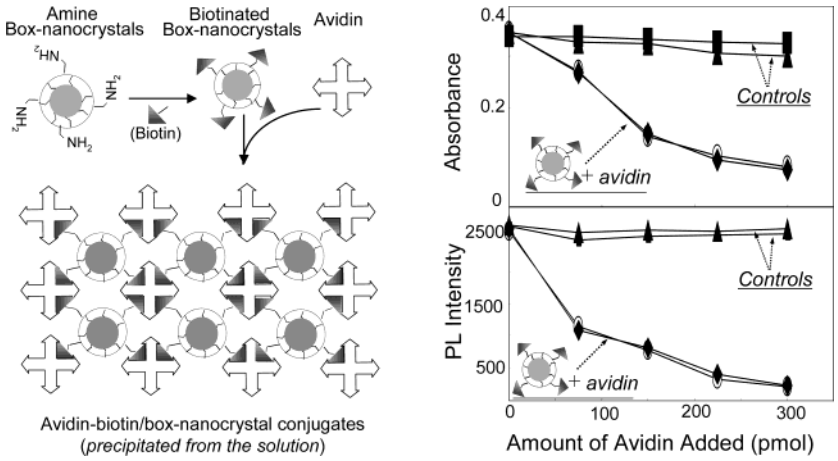

Figure 7. Left: Schematic procedure for the formation of avidin−biotin/box nanocrystal conjugates. **Right:** Quantitative results from UV−vis and PL measurements upon the formation of the conjugates. Two controls: (1) biotinlated box nanocrystals plus plain PBS buffer and (2) amine box nanocrystals plus avidin in PBS buffer.

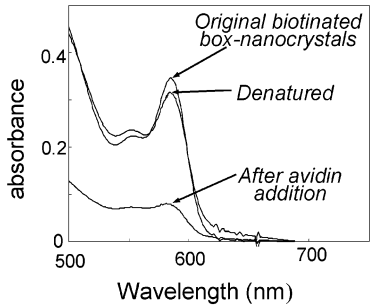

Figure 8. UV−vis spectra of the nanocrystal solutions under different conditions.

avidin and biotin. As mentioned above, the interaction between avidin and biotin like other specific bindings in biological systems is not covalent, although it is strong. If avidin is denatured by heating, the specific binding will disappear, and biotinylated nanocrystals will be released into solution. Experimentally, after the avidin−biotin/box nanocrystal conjugates in the bottom of the mother solution were heated at 70 °C for about 2 h, the color of the solution came back. UV−vis absorbance and PL intensity were almost recovered to the original values of the biotinylated box nanocrystal solution before the addition of avidin (Figure 8). This result strongly suggests that the precipitation illustrated in Figure 7 was due to the specific binding between the avidin molecules added and the biotin molecules chemically attached on the surface of the box nanocrystals.

To our knowledge, biodetections using semiconductor nanocrystals have been at a qualitative and/or nonreproducible level largely because of the instability of the nanocrystals employed. In contrast, the better stability of the noble metal nanocrystal/ligand complexes made it possible for quantitative and reproducible applications with Au nanocrystals.[28,29] Although the detection method described here is just a proof-of-principle, it reveals that quantitative and reproducible detections of biotargets will be possible using box nanocrystals. Undoubtedly, further optimization of the conditions, such as amounts and density of biotin units on each nanocrystal and concentration of biotinylated nanocrystals, will greatly improve the sensitivity.

Conclusion

In summary, functionalization and stabilization of dendron nanocrystals were achieved simultaneously by the formation of the amine box nanocrystals through a simple procedure, dendrimer bridging. The resulting amine box nanocrystals are very stable in chemically, thermally, and photochemically harsh environments. The amine groups on the surface of the box nanocrystals provide the system with a variety of simple and mild chemical coupling strategies, which foster the conjugation of the nanocrystals to biological entities. Bioconjugation and biodetection using box nanocrystals were successfully demonstrated at a quantitative and reproducible level with the avidin−biotin/box nanocrystal system. The results indicate that the amine box nanocrystals are biocompatible and bioaccessible, which differs from box nanocrystals formed by RCM.[25] Although the results shown in this work are related to CdSe/CdS core/shell nanocrystals and CdSe plain core nanocrystals, the variations of this new strategy, simultaneous functionalization and formation of box nanocrystals through dendrimer bridging, should be broadly applicable for metal, oxide, and other semiconductor nanocrystal systems. This should provide a universal and simple solution for the challenging issue in the field of colloidal nanocrystals, stabilization, and functionalization of colloidal nanocrystals, for biomedical and other applications, and for certain types of fundamental studies.

Acknowledgment. Financial support from the NSF and the University of Arkansas is acknowledged. J.J.L. is grateful for the Research Assistant Fellowship provided by the Center for Sensing Technology And Research (C-STAR) at the University of Arkansas. Y.A.W. is thankful for the support from the “seeds” program of the UA-OU Joint MRSEC.

CM034341Y

(28) Taton, T. A.; Mirkin, C. A.; Letsinger, R. L. *Science* **2000**, *289*, 1757−1760.
(29) Elghanian, R.; Storhoff, J.; Mucic, R. C.; Letsinger, R. L.; Mirkin, C. A. *Science* **1997**, *277*, 1078−1081.